RSC Advances

ROYAL SOCIETY OF CHEMISTRY

www.rsc.org/advances

Cite this: DOI: 10.1039/c0xx00000x

www.rsc.org/xxxxxx

ARTICLE TYPE

Sonochemical preparation and characterization of solid dodecyl perylene diimides/MCM-41

Xuehui Zhan,[b] Kuixin Cui,[a] Maofeng Dou,[a] Shengming Jin,[*a] Xinguo Yang[c] and Haoyuan Guan[a]

Received (in XXX, XXX) Xth XXXXXXXXX 20XX, Accepted Xth XXXXXXXXX 20XX

DOI: 10.1039/b000000x

Solid state dodecyl perylene diimide (DDPDI) fluorescent materials (DDPDI/MCM-41) with strong fluorescence were successfully prepared by incorporating the DDPDI molecules into the nanopores of MCM-41 in toluene solution with subsequent ultrasonic treatment. The solid materials were characterized by small-angle X-ray diffraction (SAXRD), high-resolution transmission electron microscope (HRTEM), ultraviolet-visible spectra (DR UV-vis), fluorescence spectra, and elemental analysis. The results indicated that the DDPDI molecules were incorporated into the mesopores of MCM-41 in the monomeric or dimeric state after ultrasonic treatment, and the DDPDI content was 41.0 (mg/g). In addition, the Stokes shift of the DDPDI in MCM-41 decreased to zero in contrast to that in toluene solution. Emission of DDPDI/MCM-41 composites splitted into two peaks at 543nm and 551nm in water, indicating that DDPDI molecules attached at internal and external surface of pore of MCM-41. Difference of spectral shift was proportional to permittivity of solvent.

1. Introduction

Perylene diimide derivates (PDIs) are well-known fluorescent dyes and have received considerable attention in organic light-emitting materials due to their brilliant colors, outstanding photochemical stability, relatively high fluorescence quantum yield ($\Phi_f \approx 1$).[1] Because of its specific molecular structures, tunable morphology of aggregated structures,[2] and photophysical and photochemical performance, PDIs are promising candidates for applications in electronic and optical devices such as field-effect transistors,[3] electrophotographic applications,[4] photovoltaic device,[5] and organic light-emitting diodes.[6] However, such high fluorescence quantum yield can be obtained only in the monomer state in dilute solution, and in the solid state or concentrated solution it would strongly be quenched due to the strong π-π aggregation, which is a great disadvantage in applications of light-emitting materials where the high fluorescence quantum yield is desired. A very attractive method of solving this problem is to mix them with polymer, but there are also a series of disadvantages such as phase separation and lower stability. On the other hand, combining PDIs with inorganic materials might be a new way of obtaining high performance light-emitting materials. A. B. Djurisic and his coworkers have demonstrated that 3,4,9,10-perylenetetra-carboxylic diimide aggregated nanoclusters grown on ZnO nanorods could exhibit a blue-white photoluminescence. [7] Dodecyl perylene diimides (DDPDI, shown in Fig. 1) was one of derivatives with alkyl chains. The DDPDI monomers in dilute CH_3Cl solution gave strong fluorescence intensity with the λ_{max} at 537 nm,[8] which would have potential applications as light-emitting materials and molecular probe if the solubility in common solvent would be increased and π-π aggregation between perylene backbones would be controllable.

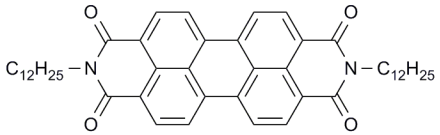

Fig. 1. Molecular structure of DDPDI.

Mesoporous materials, owing to their unique mesoporous structures, are one of the most promising hosts for incorporating host molecules into mesoporous materials to obtain functional nanocomposites. Many types of host molecules such as naphthalene and 8-hydroxyquinoline have been successfully incorporated into the mesoporous materials to form nanocomposites.[9] These composites often show unique electronic and optical characteristics, which have potential applications in optics, photonics, biosensors, and so on. Incorporating perylene diimide derivates into the mesoporous materials has also been reported in a few literatures. F.L. Castro and coworkers were the first to report that a type of perylene diimide derivates has been encapsulated into MCM-41 successfully, producing a solid red fluorescence material with an aggregates emission band at about 640 nm, which is similar to the fluorescent spectrum of PDIs assemblies. D. Li et al reported perylene bisimide derivates were incorporated into MCM-41 channel through impregnation, which resulted in red shift and broadened adsorption and emission spectra and prolonged PL lifetime compared to the molecules in CH_3Cl. [10] However, it is uncertainty that perylene diimide derivates molecules are in the pore or on the surface of MCM-41. According to mechanism of PL spectra, the peak of PL spectra should be shifted with the polarity of ambient molecules. The

stronger polarity the ambient molecules, the more red shift the PL spectra of fluorophores.

The aims of this work attempted to incorporate DDPDI molecules into 1D mesopores of MCM-41 to obtain high quantum yield of solid monomeric composites. We also attempted to develop a new method to identify the attachment site of DDPDI molecules in MCM-41.

2. Experiments

2.1 Materials and reagents

Dodecyl perylene diimide (DDPDI) was synthesized by the reaction of perylene tetracarboxylic acid bisanhydride with dodecyl amine according to the literature.[11] Cetyltrimethyl-ammonium bromide (CTAB),ethanol, and toluene were analytical grade. Water glass was from Sinopec Catalyst Company Changling Division. The silica content of water glass was 250 $g•L^{-1}$ and the module was 3.2.

2.2 Synthesis of DDPDI/MCM-41

MCM-41 was synthesized from glass water and cetyltrimethyl-ammonium bromide (CTAB) according to the following literature procedure: [12] 4.8 ml water glass was added to a solution containing 2.20 g CTAB and 60 ml deionized water. After stirring the gel formed at room temperature for 2 h, the resulting homogeneous mixture was transferred into an autoclave and kept at 373 K for 24 h. The solid products were obtained after filtering, washing, and drying at 353 K. Finally, the solid was calcined at 773 K for 5 h in the atmosphere. The BET surface area and pore size of the MCM-41 material is 907 $m^2•g^{-1}$ and 2.8nm, respectively.

The synthesis procedure of DDPDI/MCM-41 was as follows: MCM-41 was treated in vacuum for 7 h, and then the activated MCM-41 was added to the DDPDI toluene solution (the concentration of DDPDI is 4.0×10^{-4} $mol•L^{-1}$), keeping the ratios between MCM-41 and DDPDI at 1:320(g/mL). The mixture was stirred for 14 h and then the toluene was vaporized completely and the solid-state dodecyl perylene diimides fluorescence material was obtained (DDPDI/MCM-41), and the DDPDI content of the DDPDI/MCM-41 was about ca. 96.5 (mg/g). Then, the solids were dispersed in toluene, divided into two portions, and treated in an ultrasonic processing instrument (Maximum power 450 W, frequency 20 KHz, China) and mechanically agitated for 30 min twice, respectively. The samples were dried at 333 K in the atmosphere (Signed as DDPDI/MCM-41-U and DDPDI/MCM-41-M, respectively.). The DDPDI content of the DDPDI/MCM-41-U and DDPDI/MCM-41-M were calculated according to the nitrogen content that was obtained from elemental analysis. The calculation procedure was as follows:

$$C_{\mathrm{DDPDI}} = \mathrm{C_N}\frac{\mathrm{M}}{2m} \qquad (1)$$

where CDDPDI is the DDPDI content, C_N is the nitrogen content, M is the molecular weight of DDPDI, and *m* is the atomic weight of nitrogen.

2.3 Characterization of MCM-41 and DDPDI/MCM-41

Small-angle X-ray diffraction (SAXRD) patterns were obtained on a Rigaku D/max 2550 with a rotating anode and CuKα radiation at 40 kV and 300 mA; slit width of 0.25˚ and 2θ varied in the range of 1˚ to 10˚.The microstructure of MCM-41 was observed by a high-resolution transmission electron microscope (HRTEM) (Tecnai G^2 20, FEI Co.). Diffuse reflectance ultraviolet-visible spectra (DR UV-vis) were measured with a spectrometer of UV-2450 (Shimadzu, Japan), and $BaSO_4$ as an internal reference. Fluorescence spectra were measured with a spectrometer of F-4500 (Shimadzu, Japan) using excitation and emission slits of 2.5 nm and PMT voltage of 700 V. Toluene, ethanol, water, mixture of toluene and 30% ethanol, air with 50% relative humidity were applied to be solvent or ambient during fluorescence measurement. Elemental analysis was performed with a PE2400 SERIES Ⅱ CHNS/O analyzer.

3. Results and Discussion

3.1 Structure characterization

The small-angle X-ray diffraction (SAXRD) graphics of MCM-41, DDPDI/MCM-41, and DDPDI/MCM-41-U are shown in Fig. 2. Three characteristic diffraction peaks indexed to the (100), (110), and (200) diffraction are observed for the MCM-41 mesoporous materials. However, the diffraction intensity of DDPDI/MCM-41,DDPDI/MCM-41-M and DDPDI/MCM-41-U decrease slightly compared to that of the MCM-41 (Shown in inset of Fig.2.), indicating that the incorporation of the DDPDI molecules into mesopores of MCM-41 result in slight distortion of the mesoporous structure.

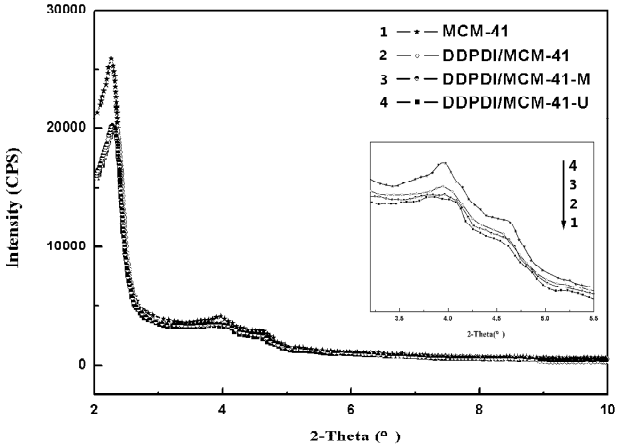

Fig. 2. XRD patterns of MCM-41, DDPDI/MCM-41,DDPDI/MCM-41-M, and DDPDI/MCM-41-U.(Inset is part presentation of XRD patterns)

Fig. 3 shows the high-resolution transmission electron microscope (HRTEM) images of MCM-41, DDPDI/MCM-41, and DDPDI/MCM-41-U, respectively. It is obvious that the MCM-41 possesses distinct one-dimension mesoporous structures (Fig.3a). However, when the DDPDI molecules are loaded, the image of DDPDI/MCM-41 shows a surface coating layer and it is difficult to distinguish the mesopores (Fig. 3b). During the incorporation process, the DDPDI molecules could be absorbed on both the internal and external surface of MCM-41 material. Some of them stacked on the surface of MCM-41 in a disordered state after the toluene was vaporized resulting in a

dark image. After ultrasonic treatment, parts of the DDPDI aggregates stacked on the outer surface were removed. As a result, the mesoporous structure became distinct again (Fig. 3c). Considering both the SAXRD and HRTEM results, it could be concluded that the mesoporous structure of MCM-41 is not destroyed by the DDPDI aggregates either on the internal surface or external surface of the pores.

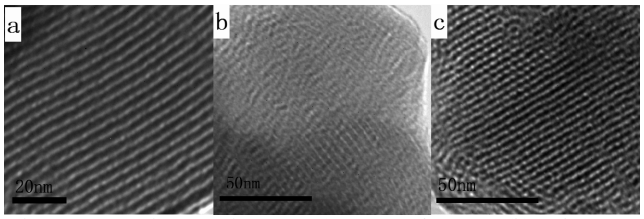

Fig. 3. HRTEM images of MCM-41(a), DDPDI/MCM-41(b) and DDPDI/MCM-41-U (c).

3.2 Fluorescence of DDPDI/MCM-41

Fig. 4 shows the DR UV-vis spectra and corresponding fluorescence spectra of DDPDI/MCM-41, DDPDI/MCM-41-U, and DDPDI/MCM-41-M together with spectra of monomeric DDPDI in toluene solution for comparison. In the toluene solution, the DDPDI molecules display a monomer UV-vis spectrum with the 0-0 transition at 527 nm and the well-resolved vibronic structure that can be ascribed to the ring-breathing vibration of the perylene skeleton. In the case of the spectrum of DDPDI absorbed on MCM-41, the absorption spectrum shifts about 10 nm for the 0-0 transition at 537 nm (Shown in inset of Fig.4).

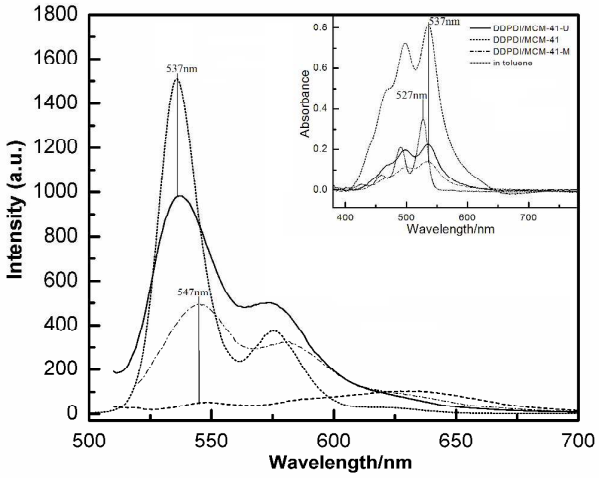

Fig.4. Fluorescence spectra of DDPDI/MCM-41 (short dash), DDPDI/MCM-41-U (solid) and DDPDI/MCM-41-M (dash dot). Fluorescence spectrum of DDPDI in toluene (2.48×10^{-5} mol·L^{-1}) (short dot) is also shown as a comparison. (Insets are corresponding UV-vis spectra of samples)

Compared to fluorescence spectrum of the monomer in the toluene solution, the fluorescence spectrum of DDPDI/MCM-41 illustrates a significant fluorescence quenching (Shown in Fig. 4). After normalization, it demonstrates a significant red shift 0-0 transition (to 547 nm) as well as a structureless broad band at 600–700 nm. This structureless broad band has same shape and peak position at different excitation wavelengths from 480 nm to 530 nm. These phenomena indicate that the aggregates have formed because of the strong intermolecular interaction. Upon photoexcitation, pronounced structure and energetic reorganization process occurs among the aggregates to form excimers.[13] Such an excimer state usually emits weakly due to the symmetry forbidden transition to the ground state.[13] Consequently, a significant fluorescence quenching and a weak structureless emission band were observed in the emission spectrum.

After ultrasonic treatment, the excimer emission band disappeared absolutely and the fluorescence intensity increased sharply (Shown in Fig. 4). Moreover, the fluorescence spectrum was similar to a monomer state spectrum with the 0-0 transition at 537 nm. These features indicate that there were no aggregates on the MCM-41 after treatment by ultrasonic waves.[14] In the ultrasonic field, through a series of compression and expansion cycles created by acoustic waves, gas bubbles appeared, grew violently, and eventually became unstable and imploded in the solution, producing high-speed acoustic streaming, intense localized heating, and high-pressure shock waves.[15] In such extreme conditions, the DDPDI aggregates were disassembled into monomers or dimers, which diffused in the mesopores and re-adsorbed on the pores' walls. In comparison, a mechanical stirring process for DDPDI/MCM-41 was carried out (Signed as DDPDI/MCM-41-M). The elemental analysis results show that the nitrogen content of DDPDI/MCM-41-U and DDPDI/MCM-41-M was 1.58 (mg/g) and 1.34 (mg/g), respectively. According to equation (1), the DDPDI contents were calculated and the results are listed in Table 1.

Table 1. DDPDI content of samples through elemental analysis

Samples	N%	DDPDI content (mg/g)
DDPDI/MCM-41	0.372	96.5
DDPDI/MCM-41-U	0.158	41.0
DDPDI/MCM-41-M	0.134	34.7

It can be seen that the DDPDI content of DDPDI/MCM-41 is comparatively higher than that of DDPDI/MCM-41-U and DDPDI/MCM-41-M. Consequently, a significant red shift of the fluorescence spectrum together was observed due to π-π interaction of the aggregation of the DDPDI molecules in large quantities. However, as shown in Fig. 4, the fluorescence spectrum of DDPDI/MCM-41-M shows an aggregate spectrum with the 0-0 transition at 547 nm, although the DDPDI content was lower than that of DDDPI/MCM-41-U. These results further prove that the ultrasonic process disassembled DDPDI aggregates into monomers or dimers. Although MCM-41 was made up of polar covalent bond, an equal force field distributed around the inner wall of pore occurred owing to symmetric structure of pore. The fluorophore of DDPDI molecules located in the pore of MCM-41 like one in nonpolar solvent.

More interestingly, after the DDPDI were incorporated into the mesopores of MCM-41, the Stokes shift decreased to zero, which was quite different from that of DDPDI in toluene. Stokes shift of DDPDI molecules was 10 nm in toluene (Shown in Fig.5a). When molecules were incorporated into the mesopores, the organic molecules were confined in the nanoscale pores and the band gap of the frontier molecular orbital was reduced resulting in a red shift of the absorption spectrum.[16] On the other

hand, in solid monomer or dimer state, the structural and energetic reorganization might not be feasible for the excited molecules due to the restriction of the finite mesopores space and the immobilization of symmetric mesoporous structure for DDPDI molecules. The same phenomena was found in rhodamine fluorophores that gas phase stokes shift was significantly smaller than that in solution phase.[17] It was similar to Stark effect spectroscopy which yielded the difference between the absorption spectrum of DDPDI in presence of an externally applied electric field and the spectrum without the electric field. The electric field acted on DDPDI in channels of MCM-41 resulted from -OH groups which symmetrically distributed on the surface of pore. In other words, the relaxation did not exist in the excited state. Therefore, although the absorption spectrum of DDPDI in MCM-41 shifted to red significantly, there is no red shift of the fluorescence spectrum, and, as a result, a zero Stokes shift of the spectrum can be observed (Shown in Fig.5b).

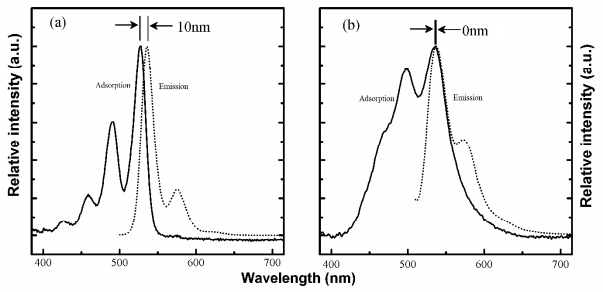

Fig.5. Normalized DR-UV-vis (solid) and fluorescence spectra (dot) of DDPDI/MCM-41-U and DDPDI in toluene.

3.3 Effects of permittivity of ambient on fluorescence of DDPDI/MCM-41-U

The solvent relaxation introduces an additional red shift to the Stokes shift of the fluorophore. Spectra of fluorophores in more polar solvents tend to be shifted more to the red. The more polarity the surrounding compounds, the larger the red shift of fluoresence. Fig.6 presents the fluorescence spectra of DDPDI/MCM-41-U in toluene, toluene with 30% ethanol, ethanol, air with 50% relative humidity and water, respectively.

The results illustrate that there is obvious red shift in fluorescence spectra of DDPDI/MCM-41-U assemblies with increase in polarity of surrounding compounds. Emission peak at 543nm, corresponding to 0-0 transition, splits into two peaks at 543nm and 551nm respectively while DDPDI/MCM-41-U composites were measured in moist air and water. It clearly indicated that there were two types of species fluorescing from different environments. As we known, fluorescence spectrum was affected by polarity and refractive index of solvent at an exact temperature through induced dipole moment of fluorophore resulting from surrounding compounds. Solvation effects were approximately described using the conductor-like screening model with the default refractive index.[18] DDPDI molecules attached in MCM-41 have two probabilities, namely, in the pore and on the outer surface of MCM-41. When DDPDI molecules were attached into the channel of molecular sieves, the molecules were in the symmetric electric field caused by hexagonal pore of MCM-41 similar to fluorophore in the nonpolar solvent. However, a small amount of polar molecules, *i.e.* H_2O and ethanol molecules, diffused into pores assembled DDPDI monomer to break the balance of force field in the pore of MCM-41. Occurrence of a limited red shift for monomers in the pore of MCM-41 was analogous to that weak polarity of solvent was executed on fluorophores. Emission peak at 543 nm was assigned to 0-0 transition of DDPDI molecules in the pore reasonably. However, water is assigned to a protic solvent which cause drastic quenching of fluorescence because of the presence of H-bonding-induced excited-state deactivation.[19] On the contrary, emission peak of DDPDI/MCM-41-U at 551nm was intensified significantly in water. This peak could be assigned to interaction between water molecules and DDPDI molecules on the surface of MCM-41. In the presence of a polarizable environment, each state corresponds to a specific collective polarization of the ambient molecules. In the case of situation that DDPDI molecules were on the outer surface of MCM-41, the collective polarization applied to fluorophores could be discomposed into asymmetric electric field on the surface of MCM-41 and the dielectric continuum of polar solvent resulted from water molecules. Additionally, steric hindrance of C_{12} hydrocarbon chains substituted for imino N site decreased the effect of protic solvent on fluorescence of mono-dispersed DDPDI molecules located outside of pore in MCM-41. It was reasonable that emission peaks at 551nm were attributed to collective electronic perturbation by -OH groups of water and surface groups of MCM-41 to the carbonyl oxygen of surface DDPDI molecules. Furthermore, we hereby proposed a method to characterize whether the guest molecules were in the pore or outside during research on host-guest assembly in porous materials.

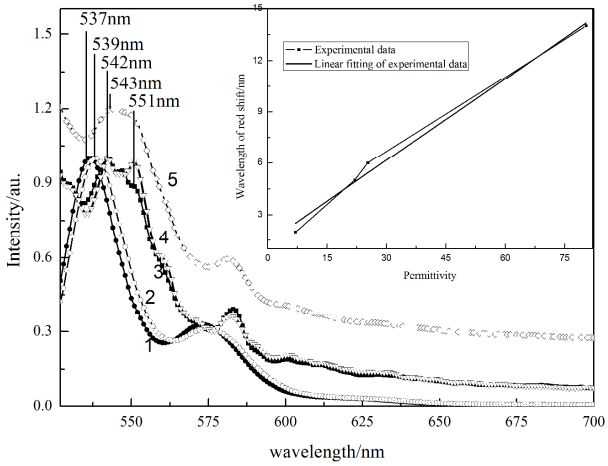

Fig.6. Normalized fluorescence spectra of DDPDI/MCM-41-U in different ambient and dependence of difference of spectral shift on permittivity of ambient (Inset).

1-Toluene;2- toluene mixed with 30% ethanol;3-Air with 50% relative humidity;4-Deionized water;5-Ethanol

As results reported by Horng et al, difference of spectral shift was directly proportional to the polarity function of environmental molecules surrounding fluorophore.[20] Polarity of surrounding compounds could be defined as dielectric constant. Dielectric constant of surrounding compounds at 20°C could be

arranged from small to large on the order of toluene (permittivity of 2.4), toluene mixture with 30% of ethanol(permittivity of 7.04), air with 50% relative humidity (permittivity of 22), ethanol (permittivity of 25.3) and water (permittivity of 80.4).[21] The linear regression fits the data to the model of following form:

$$y=0.72+0.17x$$

where y denotes the wavelength of red shift, and x is permittivity of ambient compounds (Shown in inset of Fig.6, R=0.994.). Herein a linear dependence of spectral shift on difference permittivity of ambient was observed as well. The deviation from linearity shown in figure was due to the fact that the refractive index of ambient was omitted probably.

4. Conclusions

In summary, solid monomer dispersed DDPDI/MCM-41 composite with strong fluorescence were successfully prepared through incorporation of the DDPDI molecules into the nanopores of MCM-41 in toluene solution with subsequent ultrasonic treatment. The DDPDI content of composite was 41.0 mg/g. Through cavitation and acoustic streaming of ultrasonic waves, the DDPDI aggregates in the MCM-41 could be disassembled into monomers or dimers, which presented zero Stokes shift in toluene solution. The fluorescence spectrum red shift of 0-0 transition was proportional to permittivity of ambient. Split of emission peak at 543 nm in polar ambient indicated that DDPDI molecules were attached at both sites of internal and external surface of pore of MCM-41.

Acknowledgments

Financial support of this work was provided by National Natural Science Foundation of China (51374043) and State Scholarship Fund of China (No.201206375033) .

Notes and references

[a] *School of Minerals Processing and Bioengineering, Central South University, Changsha 410083, P.R.China. Fax:+86-731-88710804; Tel:+86-731-88877204; E-mail:shmjin@csu.edu.cn*

[b] *School of Physics and Electronic Science and Engineering, Changsha University Of Science Technology, Changsha 410014, P.R.China. Tel:+86-731-85258211; E-mail: zhanxueh@163.com*

[c] *School of Materials Science and Engineering, Hunan University, Changsha 410082, P.R. China.*

1 H. Langhals, J. Karolin, L.B. Johansson, *J. Chem. Soc. Faraday Trans.* 1998, **94**,2919; S.K. Lee, Y. Zu, A. Herrmann, Y. Geerts, K. Müllen, A.J. Bard, *J. Am. Chem. Soc.* 1999,**121** ,3513; H. Quante, Y. Geerts, K. Müllen, *Chem. Mater.* 1997,**9**, 495; F. Würthner, *Chem. Commun.* 2004, 1564.

2 X.R He, W.D. Zhou, Y.L. Li, X.F. Liu, C.H. Li, H.B. Liu, D.B. Zhu, *J. Nanosci. Nanotechno.* 2008, **8**,2005; H. Weissman, A. Ustinov, E. Shimoni, S. R. Cohen, B. Rybtchinski. *Polym. Adv. Technol.* 2011, **22**, 133.

3 I. Oesterling, K. Müllen, *J. Am. Chem. Soc.* 2007,**129**,4595; M. M. Sartin, C. Huang, A. S. Marshall, N. Makarov, S. Barlow,S. R. Marder, J. W. Perry, *J. Phys. Chem. A,* 2014,**118**,110.

4 M. Guli, Y. Chen, X. Li, G. Zhu, S. Qiu, *J. Lumin.* 2007,**126**, 723.

5 E. Kozma, M. Catellani, *Dyes Pig.* 2013,**98**,160; M. R. Raj, S. Ramkumar, S. Anandan, *RSC Adv.* 2013,**3**, 5108; X. Zhang , Z. Lu , L. Ye, C. Zhan , J. Hou, S. Zhang,B. Jiang , Y. Zhao, J. Huang , S. Zhang , Y. Liu , Q. Shi , Y. Liu , J. Yao, *Adv. Mater.* 2013,**25**,579.

6 S. Li, H. Song, W. Li, X. Ren, S. Lu, G. Pan, L. Fan, H.Yu, H. Zhang, R. Qin, Q. Dai, T. Wang, *J. Phys. Chem. B.* 2006,**110**, 23164.

7 A.M.C. Ng, A.B. Djurisic, K.H. Tam, W.M. Kwok, W.K. Chan, W.Y. Tam, D.L. Phillips, K.W. Cheah, *Adv. Funct. Mater.* 2008,**18**, 566.

8 G. Boobalan, P.K.M. Imran, C. Manoharan, S. Nagarajan, *J. Colloid Interface Sci.* 2013,**393**,377.

9 S.M. Seo, E.J. Cho, S.J. Lee, K.C. Nam, S.H. Park, J.H. Jung, *Micropor. Mesopor. Mat.* 2008,**114**, 448; C. Yolanda, J.L. Beatriz, B. Cédric, V. Bruno, G. David, S. Clément, *Micropor. Mesopor. Mat.* 2007,**103**, 273; L.N. Sun, Y. Zhang, J.B. Yu, S.Y. Yu, S. Dang, C.Y. Peng, H.J. Zhang, *Micropor. Mesopor. Mat.* 2008,**115,** 535.

10 F.L. Castro, J.G. Santos, G.J.T. Fernandes, A.S. Araujo, V.J. Fernandes, M.J. Politi, S. Brochsztain, *Micropor. Mesopor. Mat.* 2007,**102**, 258; F.J. Trindade, G.J.T. Fernandes, A.S. Araújo, V.J. Fernandes Jr., B.P.G. Silva, R.Y. Nagayasu, M.J. Politi, F.L. Castro, S. Brochsztain, *Micropor. Mesopor. Mat.* 2008,**113**, 463; D. Li, Z. Tian, J. Zhang, *Res. Chem. Intermed.* 2013, **39**,1665.

11 M.J. Choi, T. Smoother, A.A. Martin, A.M. McDonagh, P.J. Maynard, C. Lennard, C. Roux, *Frensic Sci. Int.,* 2007,**173**,154.

12 K. Iwanami, H. Seo, J. Choi, T. Sakakura, H. Yasuda, *Tetrahedron*, 2010,**66**, 1898.

13 P.W. Bohn, Annu. *Rev. Phys. Chem.* 1993,**44**,37; Z. Chen, V. Stepanenko, V. Dehm, P. Prins, L.D. A. Siebbeles, J. Seibt, P. Marquetand, V. Engel, F. Wurthner, *Chem. Eur. J.* 2007,**13** ,436.

14 K. Balakrishnan, A. Datar, T. Naddo, J. Huang, R. Oitker, M. Yen, J. Zhao, L.Zang, *J. Am. Chem. Soc.* 2006,**128**, 7390.

15 L. Zhang, P. Cheng, D. Liao, *J. Chem. Phys.* 2002,**117**, 5959; L. Zhang, P. Cheng, *Phys. Chem. Comm.* 2002, **6**, 62.

16 B.S. Schueller, R.T. Yang, *Ind. Eng. Chem. Res.* 2001,**40**, 4912; P.R. Birkin, D.G. Offin, P.F. Joseph, T.G. Leighton, *J. Phys. Chem. B,* 2005,**109**, 16997.

17 A. M. Nagy, F. O. Talbot, M. F. Czar and R. A. Jockusch, *J. Photochem. Photobiol*. A, 2012, **244**, 47.

18 J.F. Greisch, M. E. Harding, M. Kordel, W. Klopper,M. M. Kappes, D. Schooss, *Phys.Chem. Chem. Phys.,* 2013,**15**, 8162; C. V. Bindhu, S. S. Harilal, *Anal. Sci.* 2001,**17**,141; I. Renge, K. Mauring, *Spectrochim. Acta A*, 2013,**102**,301.

19 J.S. Yang, G.J. Huang, Y.H. Liu, S.M. Peng, *Chem. Commun.*2008, 1344; G.J. Huang, J.H. Ho, Ch. Prabhakar, Y.H. Liu, S.M. Peng, J.S. Yang, *Org. Lett.*, 2012,**14**,5034.

20 M. L. Horng, J. A. Gardecki, A. Papazyan, M. Maroncelli, *J. Phys. Chem.* 1995,**99**,17311.

21 H. Frank, *J. Nucl. Mater.* 2003,**321**, 115; R. L. David, ed., *CRC Handbook of Chemistry and Physics, Internet Version 2005,* <http://www.hbcpnetbase.com>, CRC Press, Boca Raton, FL, 2005,section 6, pp:156-165.

Graphical abstract

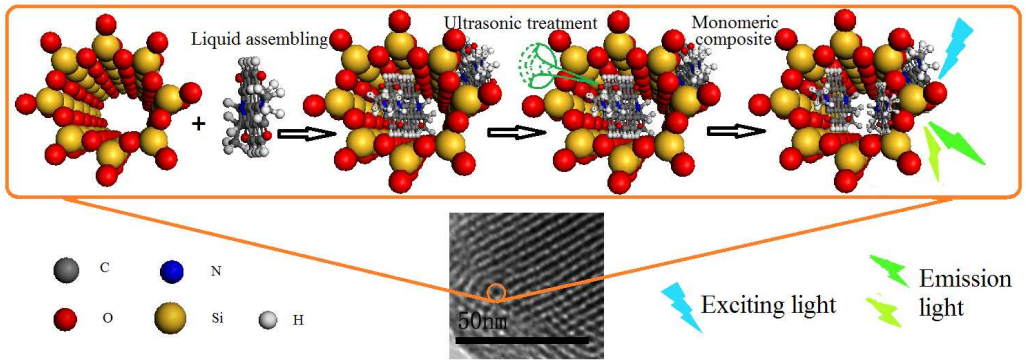

PL spectra of DDPDI/MCM-41 illustrated peak splits in protic solvent with different attachment sites of fluorophore, and linear change of red shift with permittivity of ambient after ultrasonic treatment.

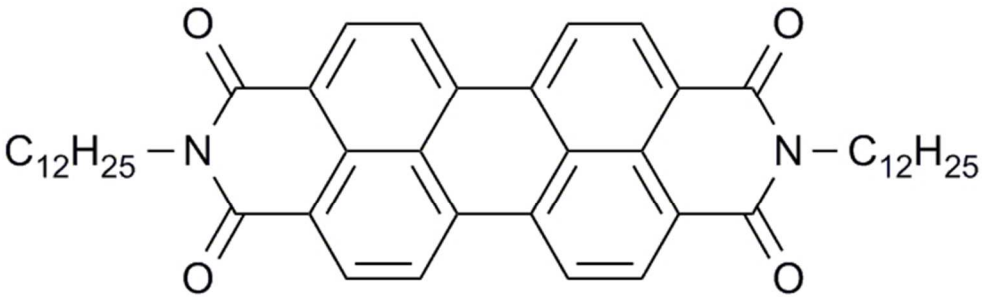

Fig.1. Molecular structure of DDPDI
58x18mm (300 x 300 DPI)

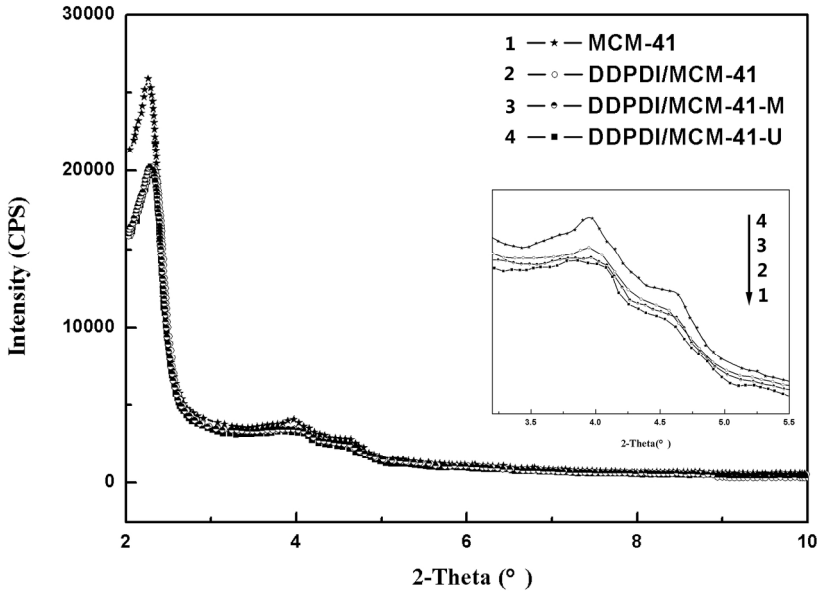

Fig.2. XRD patterns of MCM-41, DDPDI/MCM-41,DDPDI/MCM-41-M, and DDPDI/MCM-41-U.(Inset is part presentation of XRD patterns)
197x139mm (300 x 300 DPI)

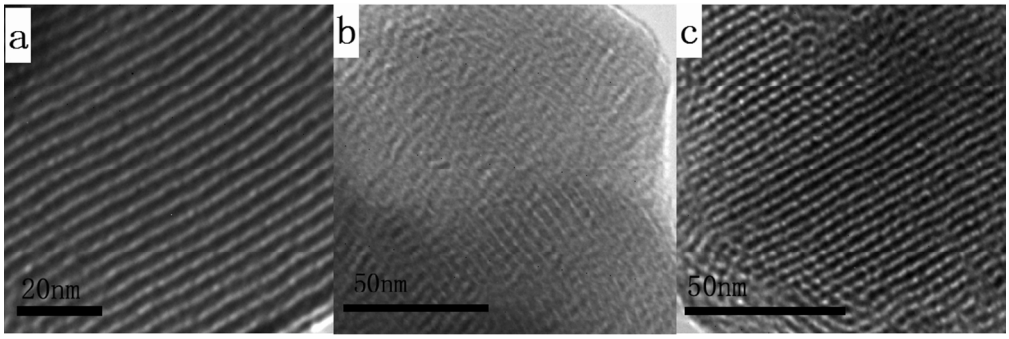

Fig. 3. HRTEM images of MCM-41(a), DDPDI/MCM-41(b) and DDPDI/MCM-41-U (c).
430x142mm (72 x 72 DPI)

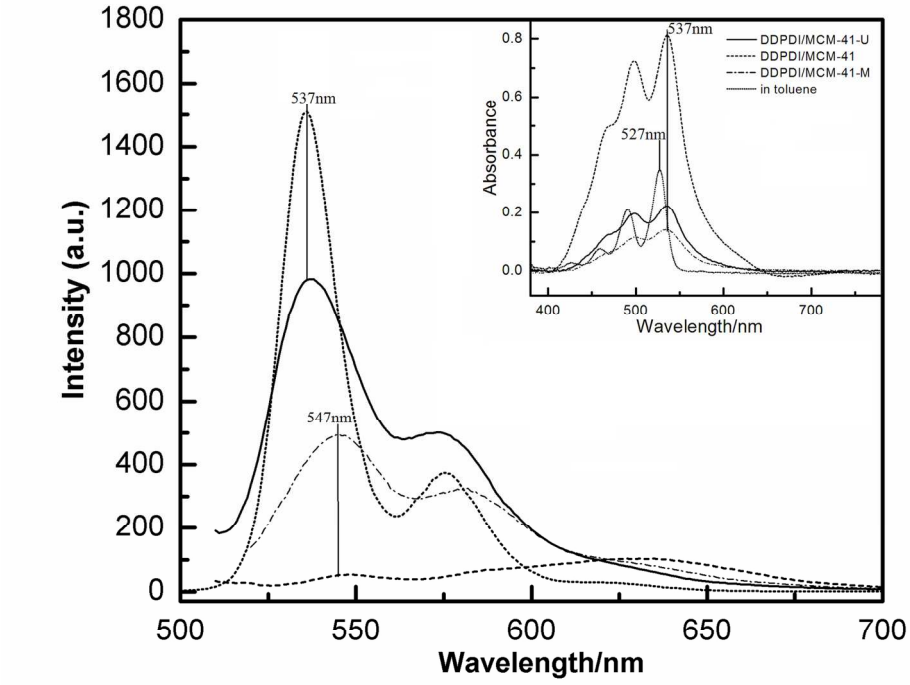

Fig.4. Fluorescence spectra of DDPDI/MCM-41 (short dash), DDPDI/MCM-41-U (solid) and DDPDI/MCM-41-M (dash dot). Fluorescence spectrum of DDPDI in toluene (2.48×10-5 mol•L-1) (short dot) is also shown as a comparison. (Insets are corresponding UV-vis spectra of samples)
165x139mm (300 x 300 DPI)

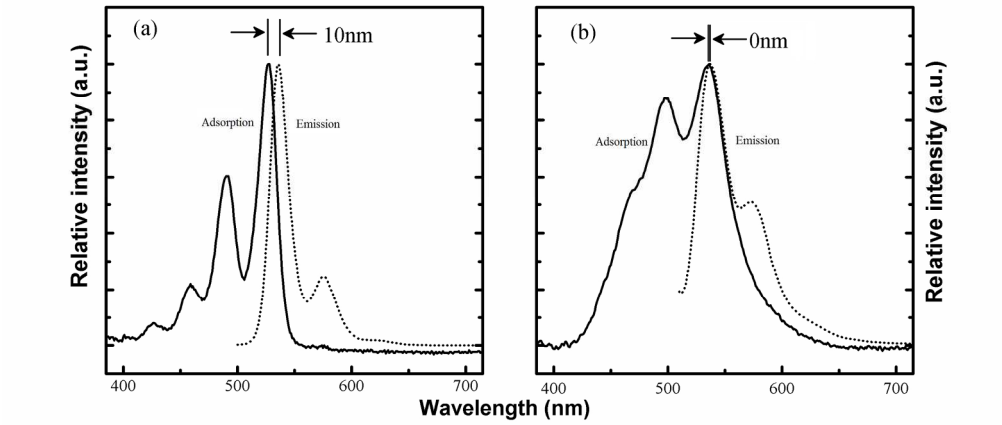

Fig.5. Normalized DR-UV-vis (solid) and fluorescence spectra (dot) of DDPDI/MCM-41-U and DDPDI in toluene.
199x119mm (300 x 300 DPI)

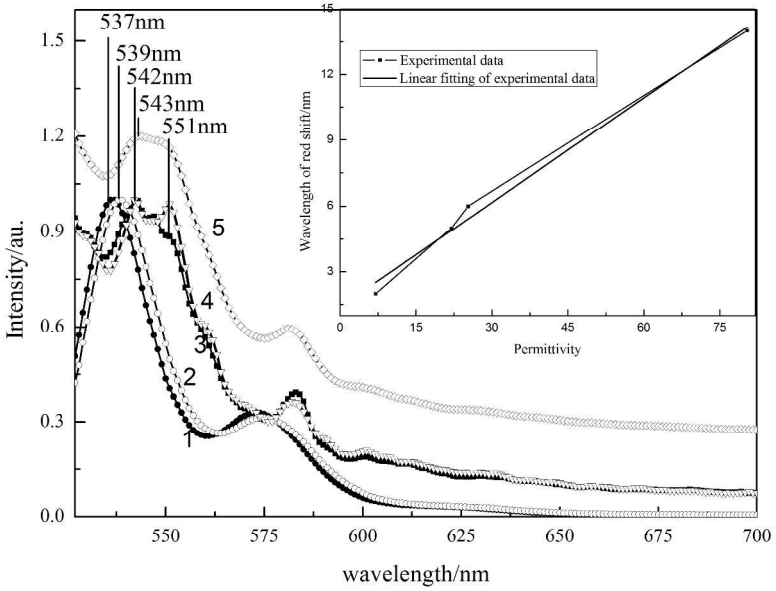

Fig.6. Normalized fluorescence spectra of DDPDI/MCM-41-U in different ambient and dependence of difference of spectral shift on permittivity of ambient (Inset).
1-Toluene;2- toluene mixed with 30% ethanol;3-Air with 50% relative humidity;4-Deionized water;5-Ethanol

289x204mm (300 x 300 DPI)